

Surface Enhanced Vibrational (IR and Raman) Spectroscopy in the Design of Chemosensors Based on Ester Functionalized *p*-*tert*-Butylcalix[4]arene Hosts

P. Leyton,[†] C. Domingo,[‡] S. Sanchez-Cortes,^{*,‡} M. Campos-Vallette,[†] and J. V. Garcia-Ramos[‡]

University of Chile, Faculty of Sciences, P.O. Box 653 Santiago, Chile, and Instituto de Estructura de la Materia, CSIC, Serrano 121, 28006 Madrid, Spain

Surface-enhanced IR (SEIR) and Raman scattering (SERS) have been employed to study the adsorption of ester functionalized *tert*-butyl calix[4]arenes on Ag and Au nanostructured surfaces as well as their complexes with pyrene. The influence of adsorption and complexation with pyrene on the host calixarene structure was tested for two different calixarene molecules bearing carboethoxy groups (CH₃CH₂COOCH₂-) in the low rim at positions 1,3- and 1,2,3,4-. The results obtained with SEIR were compared to those obtained with SERS, to better understand the interaction mechanism of the studied calixarenes with the metallic surfaces and the ligand as well as to investigate the structure/selectivity relationship of these two surface techniques in the analysis of recognition problems in which these ester functionalized calixarene molecules are involved.

Introduction

Calixarenes are synthetic cyclo-oligomers formed via a phenol–formaldehyde condensation. They exist in a “cup” like shape with a defined upper and lower rim and a central annulus (see Figure 1). Calixarenes have interesting applications as host molecules as a result of their preformed cavities.^{1,2} By changing the chemical groups of the upper and/or lower rim, it is possible to prepare different derivatives with differing selectivities to bind guest ions and molecules. Adsorption and self-assembled monolayer formation of calixarenes is a prerequisite for the application of calixarenes in sensor devices. Therefore, the study of the adsorption of these materials on a surface is a matter of importance to implement calixarene-based sensor devices. However, the adsorption and organization of calixarene molecules on substrates have been scarcely studied on metal surfaces, where charge-transfer phenomena can take place with interest for optical sensing.^{3–7}

In recent works, we have reported the surface-enhanced Raman scattering (SERS) spectra of a series of calix[4]arene derivatives on Ag colloidal surfaces and on Ag nanoparticle immobilized films.^{8,9} In these works, we have demonstrated that calixarenes can be successfully used in the detection of polycyclic aromatic hydrocarbons

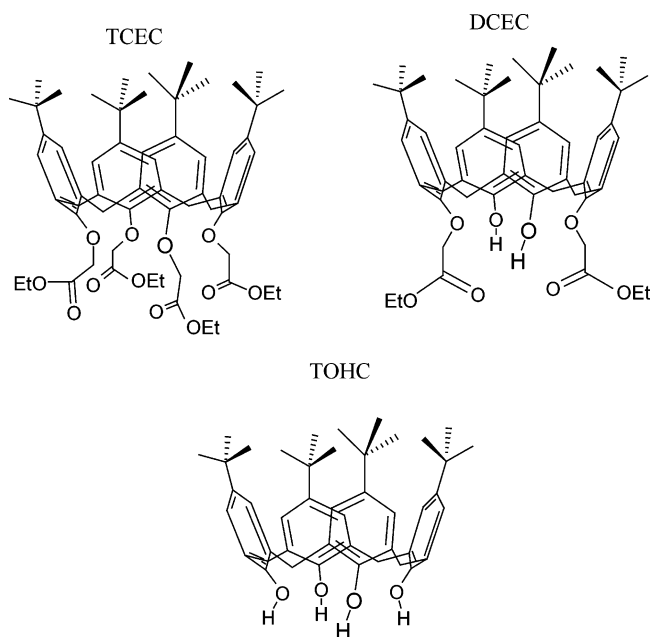


Figure 1. Calixarene structures.

(PAHs) at trace concentrations by means of SERS spectroscopy.

The detection of a molecule by SERS requires its approaching to the metal surface by some kind of interaction (physisorption or chemisorption). However, PAHs are not able to interact with the surface. The calixarene host molecule adsorbed onto the metal surface binds the PAH molecule placing it in a closer position with respect to the surface, needed for the SERS detection. Ester functionalized calix[4]arene bearing four *t*-butyl groups in the upper rim displayed a high selectivity in the

* To whom correspondence should be addressed. Fax: + 34 91 5 64 55 57. Phone: + 34 91 5 61 68 00. E-mail: imts158@iem.cfmac.csic.es.

[†] University of Chile.

[‡] Instituto de Estructura de la Materia, CSIC.

(1) Gutsche, C. D. *Calixarenes in Supramolecular Chemistry*; Stoddart, J. F., Ed.; Royal Society of Chemistry: Cambridge, U.K., 1992.

(2) Cadogan, F.; Nolan, K.; Diamond, D. *Sensor Applications in Calixarenes*; Asfari, Z., Böhmer, V., Harrowfield, J., Vicens, J., Eds.; Kluwer Academic Publishers: Dordrecht, The Netherlands, 2001.

(3) Moreira, W. C.; Dutton, P. J.; Aroca, R. *Langmuir* **1995**, *11*, 3137.

(4) Marengo, C.; Stirling, C. J.; Yarwood, J. *J. Raman Spectrosc.* **2001**, *32*, 183.

(5) Kim, J. H.; Kim, Y. G.; Lee, K. H.; Kang, S. W.; Koh, K. N. *Synth. Mater.* **2001**, *117*, 145.

(6) Zhang, M.; Anderson, M. R. *Langmuir* **1994**, *10*, 2807.

(7) Throughton, E. B.; Bain, C. D.; Whitesides G. M. *Langmuir* **1988**, *4*, 365.

(8) Leyton, P.; Sanchez-Cortes, S.; Garcia-Ramos, J. V.; Domingo, C.; Campos-Vallette, M. M.; Saitz, C.; Clavijo, R. E. *J. Phys. Chem. B* **2004**, *108*, 17484.

(9) Leyton, P.; Sanchez-Cortes, S.; Garcia-Ramos, J. V.; Domingo, C.; Campos-Vallette, M. M.; Saitz, C. *Appl. Spectrosc.* **2005**, *59*, 1009.

detection of four-ring PAH molecules.⁹ In particular, the calixarene derivative 25,27-dicarboethoxy-26,28-dihydroxy-*p*-*tert*-butylcalix[4]arene (DCEC) has been demonstrated to be the most appropriate host regarding both the sensitivity and selectivity in the PAH detection. SERS spectra of DCEC suggests that this molecule is adsorbed on the metal forming a self-assembly film on the colloidal nanoparticles and that the interaction with the PAH induces a significant change in the DCEC structure. From the analysis of the SERS spectra, useful information can be obtained about the importance of each molecular group in the calixarene affinity for PAHs and metal surfaces. The ester group of calixarene derivatives has an important role in the host anchorage onto the metal surface, and it undergoes significant structural modifications upon interaction with the PAH molecule analyte.

Since the ester groups give rise to intense IR signals, the application of surface-enhanced infrared (SEIR) should be of great help to follow in more detail changes occurring in this group.

SEIR was first developed by Osawa¹⁰ in the 1990s. The enhancement of the IR signal is explained as being the result of the enhanced optical fields at the surface of the particles when illuminated at the surface plasmon resonance frequencies.¹¹ However, the sensitivity of these surface vibrational techniques can be very different depending on the metal substrate and the molecule adsorbed on it.¹² Aroca et al. have recently reviewed the fundamentals, experimental conditions, and possible applications of SEIR.¹¹ In a recent work, we have also applied SEIR to study the interaction of nitro-PAHs on Ag and Au films.¹³

The enhancement factors can be found in SEIR in the range 10–100 at best. Despite this small enhancement compared to that of SERS (10^6), SEIR can be also used to detect monolayers of films. SEIR is a useful technique to investigate the molecular orientation on metal surfaces. In general, it can be accepted that the intensity of the normal modes having a permanent dipole moment perpendicular to the incident radiation will be the most enhanced.^{12,14}

In this work, we study the SEIR and SERS spectra of two ester functionalized calix[4]arene compounds: DCEC and 25,26,27,28-tetracarboethoxy-*p*-*tert*-butylcalix[4]arene (TCEC). We have also employed the 25,26,27,28-tetrahydroxy-*p*-*tert*-butylcalix[4]arene (TOHC), i.e., the calixarene which has no ester groups in the lower rim, to assist in the assignment of vibrational bands.

The main goal is the study of the adsorption of DCEC and TCEC on Ag and Au surfaces; the influence of the carboethoxy groups on the anchorage of the molecule on a metallic surface; and the molecular recognition ability of these molecules toward the PAH molecule pyrene (PYR) depending on their structure.

Few works have been devoted to the joint application of SEIR and SERS in surface studies. Thus, another goal of this work was the study of the SEIR with the same metallic substrates employed to get the surface-enhanced Raman spectra (SERS) in order to compare their relative effectiveness when employed in molecular recognition processes involving calixarenes. The information obtained

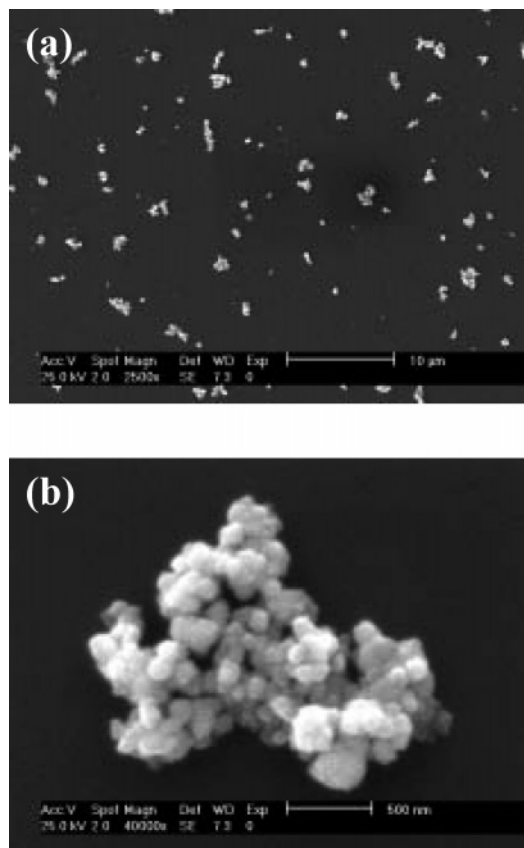


Figure 2. Micrographs of Ag/glass surface at 2500 \times (a) and 40 000 \times (b) amplification.

with these studies will be helpful in the design of sensors devices based on calixarene host molecules.

Experimental Section

Reagents. The calixarenes employed for this study were TCEC, DCEC, and TOHC (Figure 1). These calixarenes were synthesized according to described procedures.⁹ PYR was purchased from Aldrich and used as received.

Preparation of the Metal Surfaces and Samples for SEIR. Colloidal silver nanoparticles were prepared by using hydroxylamine hydrochloride as the reducing agent.¹⁵ These nanoparticles have the advantage of a more uniform distribution of size and shape together with the absence of citrate excess and its oxidation products.¹⁶ The adherence properties of these chloride-covered nanoparticles are better as concern their immobilization on glass and Ge giving rise to homogeneously distributed nanoaggregate films by a simple and direct deposition on the surface.¹⁷

Metal films of the Ag nanoparticles were prepared by a direct immobilization of colloidal Ag nanoparticles after adding aliquots of 10^{-4} M calixarene in acetone and aggregation with potassium nitrate at a 0.05 M final concentration. The Ag colloidal suspension with the calixarene was deposited on a glass slide (Ag/glass surface) and Ge (Ag/Ge surface) and dried at room temperature. The immobilized Ag nanoparticles were characterized by SEM (Figure 2) on glass, showing a uniform distribution of nanoaggregates.

Au films were prepared by metal evaporation in the following way. A total of 10 nm (mass thickness) of gold was evaporated onto polished CaF₂ and Ge windows employed as substrates. The evaporation was made in a vacuum chamber held at a pressure of 10^{-6} Torr. Film thickness was monitored using a

(10) Osawa, M. *Bull. Chem. Soc. Jpn.* **1997**, *70*, 2861.

(11) Aroca, R. F.; Ross, D.; Domingo, C. *Appl. Spectrosc.* **2004**, *58*, 324A.

(12) Sanchez-Cortes, S.; Domingo, C.; Garcia-Ramos, J. V.; Aznarez, J. A. *Langmuir* **2001**, *17*, 1157.

(13) Carrasco Flores, E.; Campos-Vallette, M. M.; Leyton, P.; Diaz Fleming, G.; Clavijo, R. E.; Garcia-Ramos, J. V.; Inostroza, N.; Domingo, C.; Sanchez-Cortes, S.; Koch, R. *J. Phys. Chem. A* **2003**, *107*, 9611.

(14) Moskovits, M. *J. Chem. Phys.* **1982**, *77*, 4408.

(15) Leopold, N.; Lendl, B. *J. Phys. Chem. B* **2003**, *107*, 2723.

(16) Sanchez-Cortes, S.; Garcia-Ramos, J. V. *J. Raman Spectrosc.* **1998**, *29*, 365.

(17) Cañamares, M. V.; Garcia-Ramos, J. V.; Gómez-Varga, J. D.; Domingo, C.; Sanchez-Cortes, S. *Langmuir* **2005**, *21*, 8546.

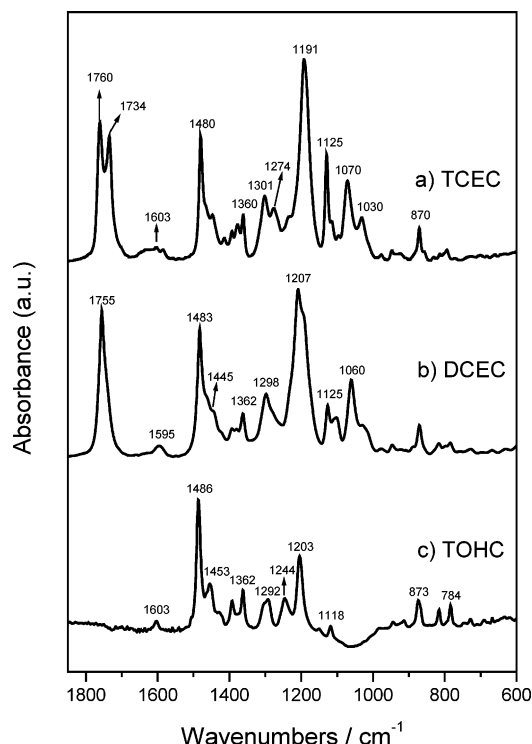


Figure 3. FTIR spectra of TCEC (a), DCEC (b), and TOHC (c) in KBr.

quartz crystal oscillator. Deposition rate was 0.65 nm/min. Samples for SEIR/SERS measurements were prepared by adding solutions of calixarenes in acetone 10^{-4} M drop by drop directly on the Au island films evaporated over germanium (Au/Ge surface) and CaF_2 substrates (Au/ CaF_2 surface). The most intense SEIR spectra were those obtained on Au/ CaF_2 surfaces.

Aliquots of the PYR dissolved in acetone (10^{-4} M) were deposited onto the calixarene-surface immobilized systems (both Ag and Au systems described above) to prepare the calixarene/PYR complexes.

Instrumentation. The SEIR spectra were measured on a FTIR Bruker IFS 66 spectrometer provided with a DTGS detector. For the polarized reflection measurements, a variable angle Reflectance accessory Specac SC19650 with a KRS5 polarizer was employed. Spectra resolution was 8 cm^{-1} and 50 scans were obtained from each sample. The overall integration time was ca. 2 min in all cases.

The SERS spectra were recorded with a Renishaw Raman Microscope System RM2000 equipped with a diode laser (providing a line at 785 nm), a Leica microscope and an electrically refrigerated CCD camera, and a notch filter to eliminate the elastic scattering. The spectra shown here were obtained by using a $100\times$ objective. The laser power in the sample was 2.0 mW. Spectral resolution was 2 cm^{-1} .

SEM micrographs were taken in an environmental scanning electron microscope (ESEM), Philips XL30 with tungsten filament operating under high vacuum mode. The acceleration voltage was 25 kV. For secondary electrons, the standard Everhard-Thornley detector was used. Samples were coated at room temperature with a 3–4 nm of gold–palladium (Au/Pd) layer using a high-resolution magnetron sputter coater operated at 800 V and 5 mA plasma current to get a coating rate of 0.5 nm/min.

Results and Discussion

Infrared Spectra in KBr. Figure 3 shows the IR spectra of all the calixarenes studied here. In Table 1, we present the main wavenumbers and the assignments according to the IR and Raman spectra of similar molecules^{3,18} and the vibrational characteristic group frequencies found in the literature.^{19,20}

Table 1. Experimental IR and SEIR Frequencies (cm^{-1}) of 25,26-Dicarboethoxy-27,28-dihydroxi-*p*-tert-butylcalix[4]arene (DCEC) in the $1800\text{--}700\text{ cm}^{-1}$ Region^a

| IR | SEIR transmission Ag/Ge | SEIR transmission Au/ CaF_2 | SEIRA Ag/glass | assignment |
|------|-------------------------|--------------------------------------|----------------|--|
| 870 | 870 | 870 | | $\rho(\text{CH}_2)/\rho(\text{CH}_3)$ (ester) |
| 1060 | 1056 | 1068 | | $\nu_{\text{al}}(\text{C}-\text{C}) + \delta(\text{C}-\text{H})$ (ester) |
| 1100 | | | | $\nu_{\text{al}}(\text{C}-\text{O}) + \delta(\text{C}-\text{H})$ (ester) |
| 1125 | 1127 | 1127 | | $\nu_{\text{al}}(\text{C}-\text{O}) + \delta(\text{C}-\text{H})$ (ester) |
| 1191 | 1187 | 1188 | | $\nu_{\text{ar}}(\text{C}-\text{O}) + \delta(\text{C}-\text{H})$ |
| 1207 | | | | $\nu_{\text{ar}}(\text{C}-\text{O}) + \delta(\text{C}-\text{H})$ |
| 1298 | 1297 | 1278 | | $\nu_{\text{ar}}(\text{C}-\text{O})$ |
| 1362 | | | 1360 | $\nu_{\text{ar}}(\text{C}-\text{O})/\delta(\text{OH})$ |
| 1445 | | | 1445 | $\delta(\text{CH}_2)$ |
| 1460 | | | | $\delta(\text{CH}_2)/\delta(\text{CH}_3)$ |
| 1483 | 1478 | 1481 | 1480 | $\delta(\text{CH}_3)$ |
| 1595 | | | 1596 | $\nu(\text{C}=\text{C})$ benzene |
| | | 1742 | 1738 | $\nu(\text{C}=\text{O})$ bounded ester |
| 1755 | | | 1759 | $\nu(\text{C}=\text{O})$ free ester |

^a Abbreviations: ν , stretching; δ , bending; ρ , rocking; ar, aromatic; al, aliphatic.

A comparative study of TCEC, DCEC, and TOHC IR spectra has been carried out in order to assist in the vibrational assignment of these molecules. The main differences seen between IR spectra of carboethoxy calixarene derivatives and TOHC are the presence of intense bands above 1700 cm^{-1} , attributed to $\nu(\text{C}=\text{O})$ stretching motions, and the bands in the $1250\text{--}1000\text{ cm}^{-1}$ region corresponding to the ester group. The strong band at 1191 cm^{-1} in TCEC, and 1207 cm^{-1} in DCEC, corresponds to that at 1203 cm^{-1} in TOHC and can be assigned to the aromatic $\nu(\text{C}-\text{O})$ ether groups which are placed in the lower rim of all of the calixarenes. The bands observed in the $1130\text{--}1000\text{ cm}^{-1}$ region must correspond to the carboethoxy $\nu(\text{C}-\text{O})$, $\nu(\text{C}-\text{C})/\delta(\text{C}-\text{H})$ vibrations, since they do not appear in TOHC, whereas the bands appearing in the $1300\text{--}1270\text{ cm}^{-1}$ region can also be assigned to aromatic $\nu(\text{C}-\text{O})$ vibrations coupled to ring stretching vibrations.

The presence of two $\nu(\text{C}=\text{O})$ bands at 1760 and 1734 cm^{-1} in the IR spectrum of TCEC suggests that two different carbonyl groups exist in this calixarene under different environments. In contrast, an intense carbonyl band at 1755 cm^{-1} is observed in the DCEC IR spectrum (Figure 3b). The doublet appearing at $1301/1274\text{ cm}^{-1}$ (in TCEC) seems to be also sensitive to the ester structure, as indicated by the presence of only one band in DCEC at 1298 cm^{-1} .

Finally, the bands appearing between 1483 and 1445 cm^{-1} are due to deformation vibrations of CH_3 and CH_2 , respectively.

Surface-Enhanced Infrared Spectra. DCEC. Figure 4 displays the transmission IR spectra of DCEC in KBr (Figure 4a) and transmission SEIR spectra of the calixarene deposited on Ag/Ge (Figure 4b), Au/ CaF_2 (Figure 4d). In the case of Ag immobilized nanoparticles, the region above 1300 cm^{-1} is difficult to analyze because of the presence of water in the sample, as deduced from the poor signal-to-noise ratio (due to the water vapor) and the broad $\delta(\text{OH}_2)$ seen at 1640 cm^{-1} .

The $\nu(\text{C}=\text{O})$ band at 1755 cm^{-1} undergoes a shift downward which is more evident on Au (Figure 4d). This suggests that the molecule is adsorbed through the ester

(18) Dormann, J.; Ruoff, A.; Schatz, J.; Vysotsky, M. O.; Bohmer, V. *J. Chem. Soc., Perkin Trans.* **2002**, 2, 83.

(19) Lin-Vien, D.; Colthup, N. B.; Fateley, W. G.; Grasselli, J. G. *The Handbook of Infrared and Raman Characteristic Frequencies of Organic Molecules*, 1st ed.; Academic Press: Boston, 1991.

(20) Socrates, G. *Infrared and Raman Characteristic Group Frequencies: Tables and Charts*; John Wiley and Sons: New York, 2001.

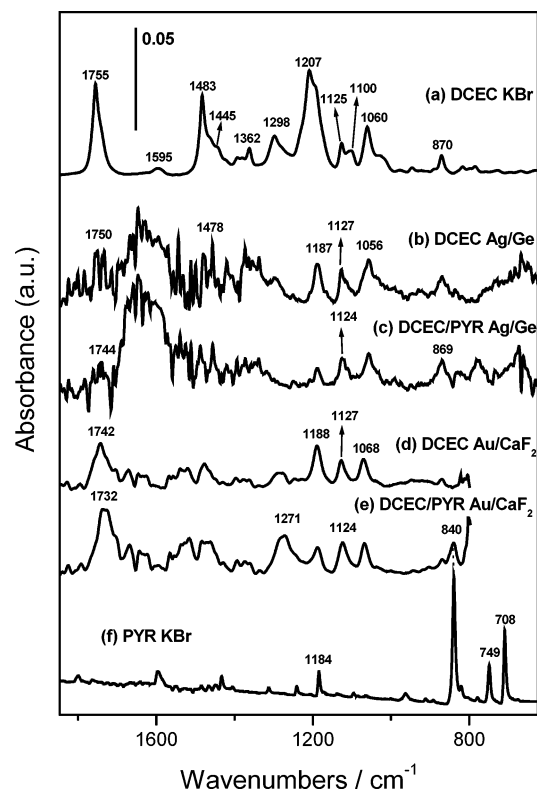


Figure 4. FTIR spectra of DCEC in KBr (a); SEIR spectrum of DCEC on Ag/Ge (b); SEIR spectrum of DCEC/PYR complex on Ag/Ge (c); SEIR spectrum of DCEC on Au/CaF₂ (d); SEIR spectrum of DCEC/PYR complex on Au/CaF₂ (e); and FTIR spectrum of PYR in KBr (f). All of the spectra were recorded in transmission.

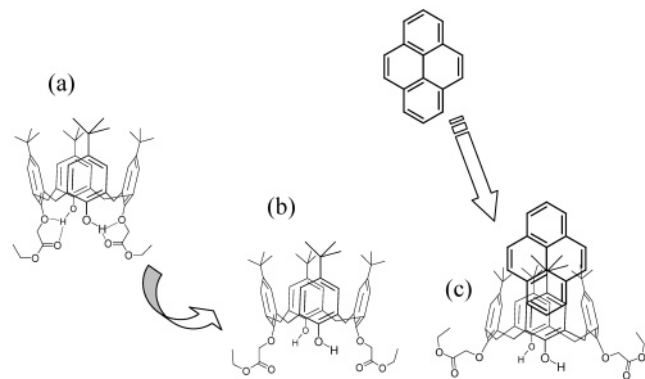


Figure 5. Suggested structural changes occurring on DCEC (a) upon adsorption on the metal surface (b) and complexation with PYR (c).

moiety on the metal. Related to this, the strong $\delta_s(\text{CH}_3)$ band of *t*-butyl groups at 1483 cm⁻¹ is weaker due to the further position of this group (Figure 5b) with respect to the surface.

DCEC in KBr displays doublets at 1207/1188, 1125/1100, and 1060/1050 cm⁻¹ in the IR spectrum (Figure 4a). However, when this calixarene is adsorbed on Ag (Figure 4b) and Au (Figure 4d), prominent bands are seen at 1187, 1127, and 1056 cm⁻¹ on Ag and at 1188, 1127, and 1068 cm⁻¹ on Au, indicating that clear structural changes occur upon adsorption on the surface. In addition, the upward shift of the ester $\nu(\text{C}-\text{O})$ band from 1125 to 1127 cm⁻¹ and its intensity increase are related to the shift downward of the $\nu(\text{C}=\text{O})$ ester vibration. The inverse shifts observed

for the ester $\nu(\text{C}-\text{O})$ and $\nu(\text{C}=\text{O})$ motions indicates that both oxygen groups are interacting with the metal surface through a bidentate complex, as shown in Figure 5b, due to the electric charge delocalization occurring in the ester group. Moreover, this interaction induces a rearrangement of the lower molecular rim, responsible for the wavenumber shifts of 1298, 1207, and 1060 cm⁻¹ bands. The structural change probably implies a breakdown of H bonds existing in solid DCEC^{21,22} (Figure 5a) and a rearrangement of the carboethoxy group to allow a bidentate DCEC–metal interaction.

The enhancement of the 870 cm⁻¹ band on Ag is also related to the ester approach to the surface, as this band is assigned to rocking bands of CH₃ and CH₂ groups.

The $\nu(\text{C}-\text{O})$ band at 1207 cm⁻¹ seems to be very sensitive to calixarene structural changes involving the aromatic $\nu(\text{C}-\text{O})$ ether bond through which the carboethoxy group is linked to phenyl rings. This band appears at a lower wavenumber value in TCEC (Figure 3), in comparison to DCEC, due to a more open structure adopted by the four carboethoxy groups in the lower rim of the calixarene induced by the steric hindrance between them. Thus, the shift toward lower wavenumbers in DCEC when adsorbed on the metal can be also interpreted as being due to an opening of the carboethoxy groups in the lower rim (Figure 5b) in order to facilitate the bidentate interaction of DCEC with the surface.

SEIR spectra of the DCEC/PYR complex on Ag and Au are displayed in Figure 4, panels c and e, respectively. The appearance of the most intense PYR band at 840 cm⁻¹ in the Au/CaF₂/DCEC SEIR spectrum is an evidence of the DCEC/PYR interaction. The presence of PYR induces general frequency shifts, mainly in bands involving carboethoxy groups. In addition, the interaction of the calixarene with the surface is considerably affected by the analyte inclusion. The $\nu(\text{C}=\text{O})$ band at 1742 cm⁻¹ in the Au/CaF₂/DCEC surface shifts to 1732 cm⁻¹, whereas the $\nu(\text{C}-\text{O})$ band at 1127 cm⁻¹ shifts downward to 1124 cm⁻¹ both on Ag and on Au. Moreover, the $\nu(\text{C}-\text{O})$ ether aromatic band at 1188 cm⁻¹ is weakened and that at 1298 cm⁻¹ shifts downward to 1271 cm⁻¹. These changes suggest a stronger interaction of carbonyl groups and a weaker one of the C–O group in the presence of PYR toward a rather monodentate interaction (Figure 5c). This is attributed to a further opening of the carboethoxy groups in the lower calixarene rim induced by the interaction with PYR. The induced structural change also influences the ether C–O bonds of the aromatic moiety, which could adopt a less perpendicular orientation, thus explaining the 1298 → 1271 cm⁻¹ shift and the intensity decrease of the 1188 cm⁻¹ band.

The structural changes undergone by DCEC upon adsorption and interaction with PYR are also manifested in the C–H stretching region (Figure 6). A relative intensity decrease is seen for the band at 2958 cm⁻¹ both on Ag (Figure 6b) and Au (Figure 6d). On the other hand, the interaction with PYR induces an intensity increase of the band at 2917 cm⁻¹ on Ag (Figure 6c) and 2919 cm⁻¹ on Au (Figure 6e). The changes observed in this region are attributed to the reorientation of the molecule on the surface due to its complexation with PYR. In fact, the most enhanced bands must correspond to C–H stretching vibrations with preferential perpendicular orientation with respect to the surface, according to the SEIR selection rules.¹⁰

(21) Rudkevich, D. M.; Rebek, J., Jr. *Eur. J. Org. Chem.* **1999**, 1991, 1.

(22) Rudkevich, D. M. *Chem. Eur. J.* **2000**, 6, 2679.

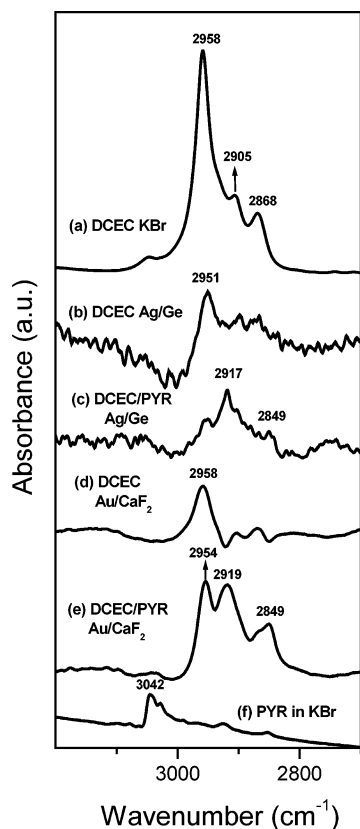


Figure 6. FTIR spectra of DCEC in KBr (a); SEIR spectrum of DCEC on Ag/Ge (b); SEIR spectrum of DCEC/PYR complex on Ag/Ge (c); SEIR spectrum of DCEC on Au/CaF₂ (d); SEIR spectrum of DCEC/PYR complex on Au/CaF₂ (e); and FTIR spectrum of PYR in KBr (f). All of the spectra were recorded in transmission in the 3200–2700 cm⁻¹ region.

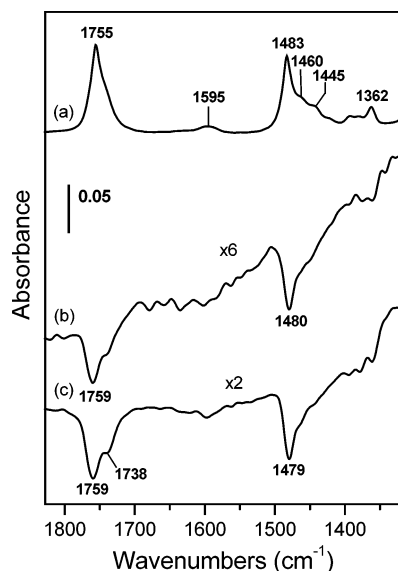


Figure 7. Transmission FTIR spectrum of DCEC in KBr (a); SEIRA (surface-enhanced infrared reflection–absorption) spectra of DCEC (b) and of DCEC/PYR complex on Ag/glass. The reflection–absorption spectra were recorded at 76° and using the s polarization.

SEIR spectra of DCEC and DCEC/PYR complex were also obtained when the Ag colloid was immobilized on glass (Figure 7) in a reflection–absorption configuration. In this case, an inversion in the absorbance peaks is observed above 1300 cm⁻¹ due to the change in the refractive index.^{23,24} The spectra displayed in Figure 7 were obtained

by using s-polarized light because the p-polarized one leads to a higher absorption of light which overlaps the calixarene absorbance bands. The changes occurring in the 1300–1000 cm⁻¹ region are very similar to those seen on Au/Ge. Unfortunately, the peak inversion in this region avoids a good observation of IR bands. Anyway, the peaks observed in the 1750–1300 cm⁻¹ region are less affected by water vapor than on Ag/Ge, because of the higher SEIR effect observed on the nanoparticles immobilized on glass. In particular, the bands corresponding to the *t*-butyl, (1483–1445 cm⁻¹), the aromatic (1596 cm⁻¹), and the ester groups (1755 cm⁻¹) appear with a high absorbance.

These bands are crucial to understand the adsorption and interaction of DCEC on Ag. The $\nu(\text{C}=\text{O})$ band, which appears at 1755 cm⁻¹ in KBr, splits into two bands at 1759 and 1738 cm⁻¹ when DCEC is adsorbed on the metal surface (Figure 7b). The lower peak may correspond to ester groups interacting with the metal, whereas the upper one could be due to free ester groups. The existence of nonbonded ester groups is probably due to the formation of multilayers on this surface. The slight shift toward higher wavenumbers (to 1759 cm⁻¹) seen in free DCEC could be attributed to the H bonds (established between C=O and the adjacent OH groups, Figure 5a) breakdown, induced by the calixarene adsorption on the metal (Figure 5b) as mentioned above. In addition, the butyl $\delta(\text{CH}_3)$ band at 1483 cm⁻¹ undergo a shift downward, suggesting a structural change of these groups upon adsorption on the surface.

The interaction with PYR (Figure 7c) induces an increase of the lower component of $\nu(\text{C}=\text{O})$ band seen at 1738 cm⁻¹, thus indicating a strengthening of the DCEC interaction with Ag. The influence of PYR is also evident on the *t*-butyl groups, since a marked intensity decrease of the shoulders at about 1460 and 1445 cm⁻¹ occurs. This indicates that PYR induces a structural change on *t*-butyl groups due to its interaction with them, which also affect the interaction of DCEC with the metal through the C=O bond of the ester group as depicted in Figure 5.

TCEC. Figure 8 displays the transmission IR spectrum of TCEC in KBr (Figure 8a) and the SEIR spectrum of the compound deposited onto a Ag/Ge surface (Figure 8b). The relative intensity and frequency changes of the $\nu(\text{C}=\text{O})$ bands indicate that the adsorbate–substrate interaction is taking place through this group. The fact that only one $\nu(\text{C}=\text{O})$ band appears at 1741 cm⁻¹ on the surface indicates the existence of a unique carbonyl structure on the surface in contrast to what happens in KBr, where two $\nu(\text{C}=\text{O})$ bands are seen at 1760 and 1734 cm⁻¹. This interaction explains why the *t*-butyl $\delta(\text{CH}_3)$ band at 1480 cm⁻¹ observed in the IR spectrum of TCEC in KBr is weaker in the SEIR spectrum due to a further position of these groups when the molecule is adsorbed through the ester groups.

The changes undergone by the $\nu(\text{C}=\text{O})$ band and those seen for the ester bands falling in the 1250–950 cm⁻¹ region support that TCEC interacts with the metal surface through this group as in the case of DCEC. In particular the most intense $\nu(\text{C}-\text{O})$ band at 1191 cm⁻¹ undergoes a significant intensity decrease and shift to 1184 cm⁻¹, whereas the band at 1128 cm⁻¹ shifts to 1124 cm⁻¹. However, the changes are not so strong as in the case of DCEC. Furthermore, the strong bands appearing at 1571 and 780 cm⁻¹ could indicate the perpendicular orientation of benzene residues with respect to the surface.⁵

(23) Bradford, D. C.; Hutter, E.; Assiongon, K. A.; Fendler, J. H.; Roy, D. *J. Phys. Chem. B* **2004**, *108*, 17523.

(24) Mielczarski, J. A.; Yoon, R. H. *J. Phys. Chem.* **1989**, *93*, 2034.

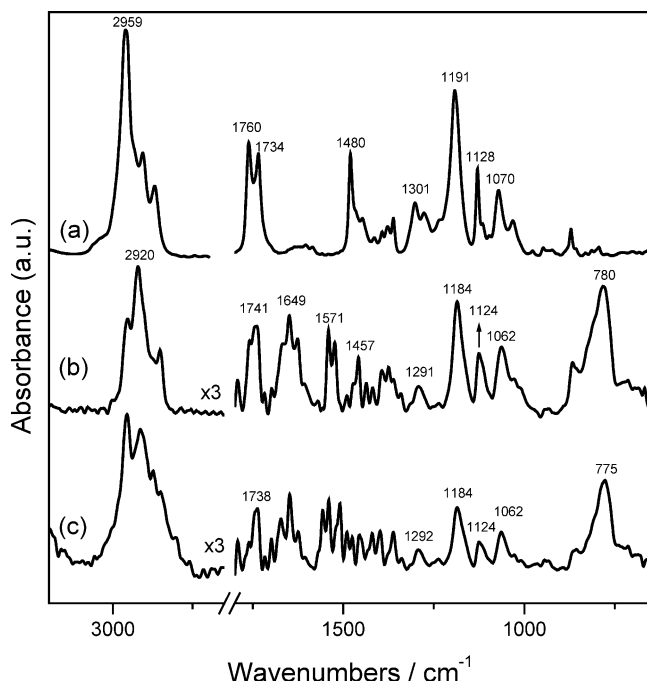


Figure 8. FTIR spectra of TCEC in KBr (a); SEIR spectrum of TCEC on Ag/Ge (b); and SEIR spectrum of TCEC/PYR complex on Ag/Ge (c).

The stretching C–H region also displays significant spectral changes when TCEC is adsorbed on the metal. The main changes are the intensity decrease of the band at 2959 cm^{-1} and the enhancement of the band at 2920 cm^{-1} . These changes can be attributed to the selection rules of SEIR, which predict a higher enhancement for those vibrational modes developing perpendicular to the surface as in the case of DCEC. Therefore, the band at 2920 cm^{-1} may correspond to C–H stretching motions of CH_2 or CH_3 groups which are predominantly oriented perpendicular with respect to the surface.

Interestingly, the spectral profile of the C–H stretching region is very similar to that found for the DCEC/PYR complex (Figure 3), since also in DCEC a prominent band at 2019 cm^{-1} is seen in the complex with PYR. Other similarities between the SEIR spectra of TCEC and DCEC/PYR complex are found in the lower wavenumber region, mainly corresponding to the position of bands at 1741 , 1184 , and 1124 cm^{-1} bands.

The similarity found between the SEIR spectrum of TCEC and that of the DCEC/PYR complex could be the key to understanding why TCEC is less active binding PAHs molecules, as demonstrated in previous experiments.⁸ In fact, both the steric hindrance of carboethoxy groups and the interaction with the metal may induce a shutdown of the calixarene upper rim, which may prevent the inclusion of PYR. This structural change does not occur in DCEC, due to the lower steric effect of the two carboethoxy groups. Nevertheless, the interaction of DCEC with PYR could lead to a shutdown of the upper rim and an opening of the calixarene lower rim, as depicted in Figure 5c, similar to that occurring for noncomplexed TCEC.

The addition of PYR has a poor influence on the structural marker bands of TCEC (see the $1300\text{--}1000\text{ cm}^{-1}$ region in Figure 8c). However, PYR induces a clear change in the C–H stretching region and the weakening of the 1457 cm^{-1} band. Thus, we suggest that TCEC interacts weakly with PYR through the *t*-butyl groups of the upper calixarene rim, although this interaction is much

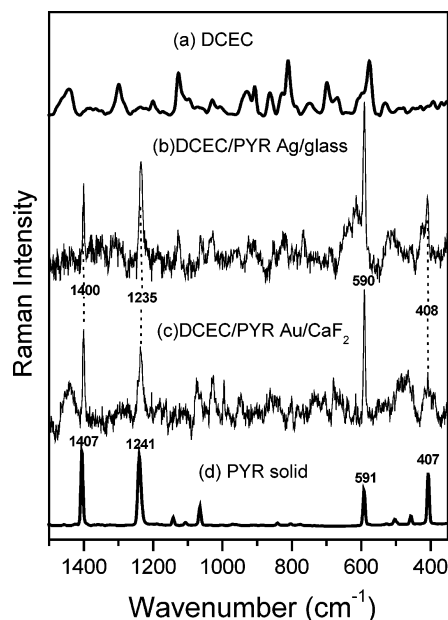


Figure 9. Raman spectrum of solid DCEC (a); SERS spectrum of DCEC/PYR complex on Ag/glass (b) and on Au/CaF₂ (c); and Raman spectrum of PYR in solid state (d). Excitation wavelength at 785 nm .

weaker than that observed for DCEC, having a lower influence in the ester bands.

Surface-Enhanced Raman Spectra of DCEC. Figure 9, panels b and c, displays the SERS spectrum of the DCEC/PYR complex on the same Ag/glass and Au/CaF₂ surface employed to obtain the SEIR spectra, compared to the Raman of calixarene (Figure 9a) and that of PYR (Figure 9d). In contrast to the SEIR spectrum, which is dominated by the IR absorption bands corresponding to the calixarene, the SERS spectrum shows intense PYR bands at 1400 and 1235 cm^{-1} which corresponds to the bands at 1407 and 1241 cm^{-1} in the solid, and which are assigned to in-plane ring stretching motions and in-plane $\delta(\text{C-H})$ vibrations.²⁵ The shift downward of the latter bands is attributed to the interaction with calixarene.⁸ Moreover, a marked enhancement of the band at 590 cm^{-1} and an intensity decrease of that at 408 cm^{-1} are observed. In general, all of the intensified bands correspond to symmetric a_g modes,^{25–27} which are enhanced through a Franck–Condon resonance mechanism,²⁸ most probably associated to a charge-transfer in the complex-surface system, as it also occurs for naphthalene interacting with TOHC.²⁹

Conclusions

SEIR spectroscopy is an important technique in the study of the adsorption of ester functionalized host molecules calix[4]arene on metallic surfaces. The interaction of these molecules with Ag and Au surfaces takes place through the ester groups. Thus, since the ester vibrational bands are very intense in IR absorption spectroscopy, the SEIR technique is an ideal technique to follow the adsorption of these molecules in the studied

(25) Carrasco, E. A.; Clavijo, R. E.; Campos-Vallette, M.; Leyton P.; Diaz, G.; Koch, R. *Vib. Spectrosc.* **2004**, *37*, 153.

(26) Hudgins, D. M.; Sandford, S. A. *J. Phys. Chem. A* **1998**, *102*, 329.

(27) Shinohara, H.; Yamakita, Y.; Ohno, K. *J. Mol. Struct.* **1998**, *442*, 221.

(28) Creighton, J. A. *The Selection Rules for Surface-enhanced Raman Spectroscopy in Spectroscopy of Surfaces*; Clark, R. J. H., Hester, R. E., Eds.; John Wiley & Sons: Chichester, U.K., 1988; p 76.

(29) Kook, S. K. *Bull. Korean Chem. Soc.* **2002**, *23*, 111.

substrates. Structural marker bands were identified to follow the changes occurring in these molecules

SEIR spectra have demonstrated the existence of remarkable differences between the adsorption behavior of ester functionalized calix[4]arenes depending on the substitution pattern of the lower rim. DCEC, with a 1,3-dicarboethoxy substitution, is anchored on both Ag and Au films through a bidentate interaction. An opening of the lower rim is induced in order to better accommodate the ester groups toward the surface. SEIR technique has also demonstrated that the interaction of DCEC with metals seems to take place more strongly on Au than on Ag.

The adsorbed DCEC displays an appropriate conformation to interact with PAHs analytes such as pyrene. However, TCEC ester groups are linked to the surface through a monodentate interaction due to the more open conformation in its lower rim, constrained by the steric hindrance of the carboethoxy groups. This fact seriously limits its possible use in the detection of PYR and other PAHs. On the other hand, the interaction of DCEC with PYR leads to significant structural changes mainly affecting the carboethoxy union with the metal, which can be also easily deduced by SEIR.

The comparison between SEIR and SERS indicates that both techniques are complementary, since each one affords different information on the DCEC/PYR complex. SERS spectra are mainly dominated by PYR bands. Thus, SERS can be used to follow the changes occurring in the PAHs as a consequence of the interaction with the calixarene host and for detection purposes.

In contrast, SEIR spectra display more intense bands corresponding to the more polar groups existing in the

calixarene host molecule. This makes this technique appropriate to follow structural changes occurring due to the adsorption and the complexation with the analyte and to find a structure/selectivity relationship. In the case of the DCEC vs TCEC comparison, the SEIR spectra gave the key to understand why the TCEC calixarene is less active in the PAHs detection, which can be attributed to a shutdown of the *t*-butyl groups in the upper calixarene rim.

Finally, the influence of the SEIR/SERS substrate on the pollutant detection is of interest, as revealed by comparing the SEIR spectra of Ag immobilized on glass or on Ge. In fact, the carbonyl ester and *t*-butyl groups are better seen on Ag nanoparticles immobilized on glass, due to its higher effectiveness regarding the SEIR enhancement. In this sense, we have demonstrated that simple SEIR substrates can be fabricated, at low cost, by immobilizing Ag nanoparticles obtained by conventional procedures on easily available materials such as glass which can act as very effective substrates either for SERS or SEIR spectroscopies.

Acknowledgment. Authors acknowledge project Fondecyt 1040640 from Conicyt (Chile), Fundacion Los Andes project C-13879, the Convenio Conicyt/CSIC 2003/2004 and Grant FIS2004-00108 from Dirección General de Investigación, Ministerio de Educación y Ciencia and Comunidad Autonoma de Madrid Project No. GR/MAT/0439/2004 for financial support. P.L. acknowledges Project AT 4040084 from Conicyt.